Supplementary Information

Densely-distributed Co onto carbon-layer coated flower-like Ni/Al_2O_3 and later integration into stirrer for multiple catalytic degradation and solar-powered water evaporation

Shuang Jiang[1], Hongyao Zhao[1], Zichen Ma, Hongyang zhu, Danhong Shang, Linzhi Zhai, Yanyun Wang*, Yiyan Song*, Fu Yang*

School of Environmental and Chemical Engineering, Jiangsu University of Science and Technology, Zhenjiang 212003, China
Prof. Fu Yang, e-mail: *fuyang@just.edu.cn,* Dr. Yanyun Wang, e-mail: *wangyanyun@just.edu.cn*

Y.Y. Song*
Department of Clinical Laboratory, The Fifth People's Hospital of Suzhou, The Affiliated Infectious Diseases Hospital of Soochow University, Suzhou, 215000, China
e-mail: *songyiyan94@163.com*

[1]These author equally contributed to this work.

Photothermal experiment operation description

Initially, an appropriate amount of water was poured into a flat beaker. To prevent radiative heat loss from the evaporating heat to the water body, thermal insulation foam to isolate the lower water body and the upper evaporation layer was used. A root system was utilized to pump water upwards. The top evaporation layer and photothermal membrane were placed at the center. To minimize heat radiation loss, the beaker was also encased with thermal insulation foam. Subsequently, the light intensity of the simulated sunlight device covering the top of the evaporation device was adjusted to match sunlight intensity, placed on a precise balance. As the surface temperature of the membrane rapidly rose and steam overflow gradually, evaporation increased over time, resulting in a gradual decreasing weight of the overall evaporation device. The weight of device was recorded at specified intervals, and the weight loss was calculated to determine the photothermal membrane evaporation efficiency. The solar steam experiment was conducted based on a solar evaporator involved a system containing simulated sunlight illumination, an analytical balance tracked steam production, an infrared camera monitoring temperature changes and a light meter measuring light intensity. The room temperature remained between 19-25 °C, and humidity levels maintained at 70 %.

The heat loss during solar steam generation consists of three components including radiation, convection, and conduction. A detailed analysis of these components is as follows.

Radiation component

Thermal radiation loss is calculated by the Stefan-Boltzmann equation,

$$\emptyset = \varepsilon \ A \ T\sigma_1^4 - (T_2^4)$$

Φ represents the heat flux, ε is the emissivity and the value is 1. A is the effective evaporation surface area (225 mm^2), and σ is the Stephen Boltzmann constant (5.67×10^{-8} $W\cdot m^{-2}\cdot K^{-4}$). The surface temperature of the membrane after T_1 is stably evaporated under sunlight (about 40.8 °C, namely 313.95 K), and T_2 is the ambient

temperature above the membrane. So the thermal radiation of $Ni/Al_2O_3@Co_{500}$ membrane is calculated and the calculated thermal radiation loss is 2.7 %.

Convection component

Convective heat loss is defined by Newton's law of cooling and the formula is shown as follows,

$$Q = hA\Delta T$$

Q represents the convective heat flux, h is the convective heat transfer coefficient about 5 $W \cdot m^{-2} \cdot K^{-1}$. And A denoting the effective evaporation surface area is about 225 mm^2. ΔT is the difference between the surface temperature of the prepared solar evaporation material and the ambient temperature. Therefore, the convective heat loss of the $Ni/Al_2O_3@Co_{500}$ membrane is calculated to be 2.1 %.

Conduction component

The thermal conduction heat loss is caused by the heat transferred from the prepared material to the water, and the calculation formula is as follows,

$$q = kA\frac{(T_1 - T_2)}{L}$$

In the formula, q represents the heat transfer, because it is made of foam for thermal insulation. And k is the thermal conductivity of foam about 0.03 $W \cdot m^{-1} \cdot K^{-1}$. A representing the heat exchange surface area is about 225 mm^2. T_1 and T_2 are the surface temperature of the prepared solar evaporation material and the ambient temperature after the steady-state temperature, respectively. L is the thickness of foam support (13 mm). Therefore, according to the formula, the thermal conduction heat loss of $Ni/Al_2O_3@Co_{500}$ membrane is calculated to be 0.9 %.

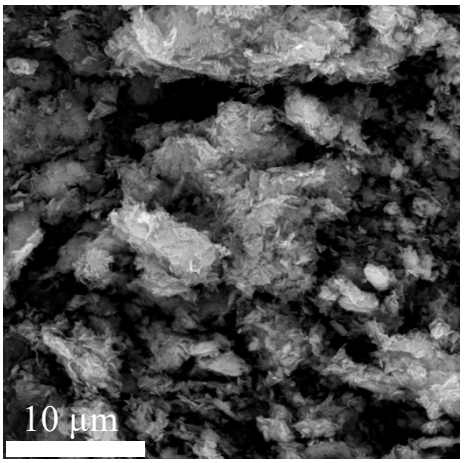

Figure S1. Representative SEM image of the Al_2O_3@Co_{500}.

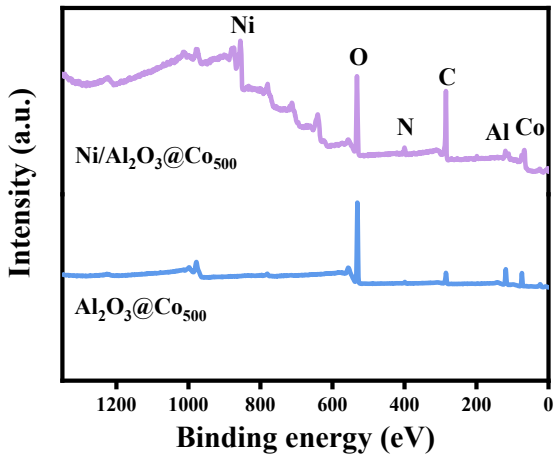

Figure S2. X-ray diffraction photoelectron spectroscopy (XPS) surveys of Ni/Al_2O_3@Co_{500} and Al_2O_3@Co_{500}.

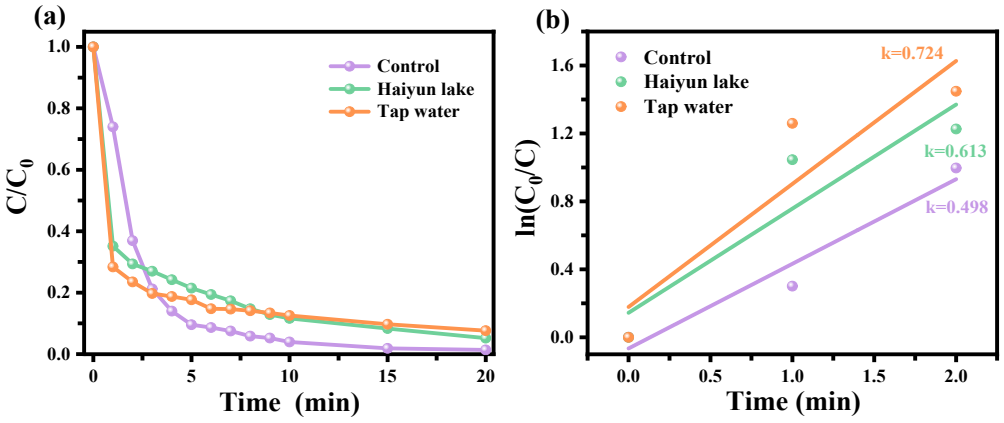

Figure S3. (a) Time-dependent TC degradation curves and (b) corresponding kinetic curves of $ln(C_0/C)$ with reaction time on Ni/Al_2O_3@Co_{500} in different actual water sources.

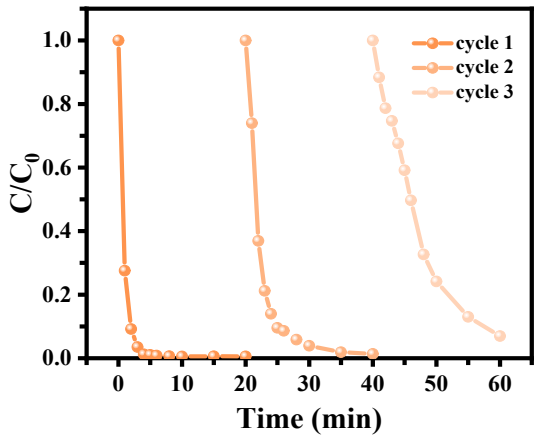

Figure S4. Three consecutive TC degradation cycles test of $Ni/Al_2O_3@Co_{500}$ catalyst.

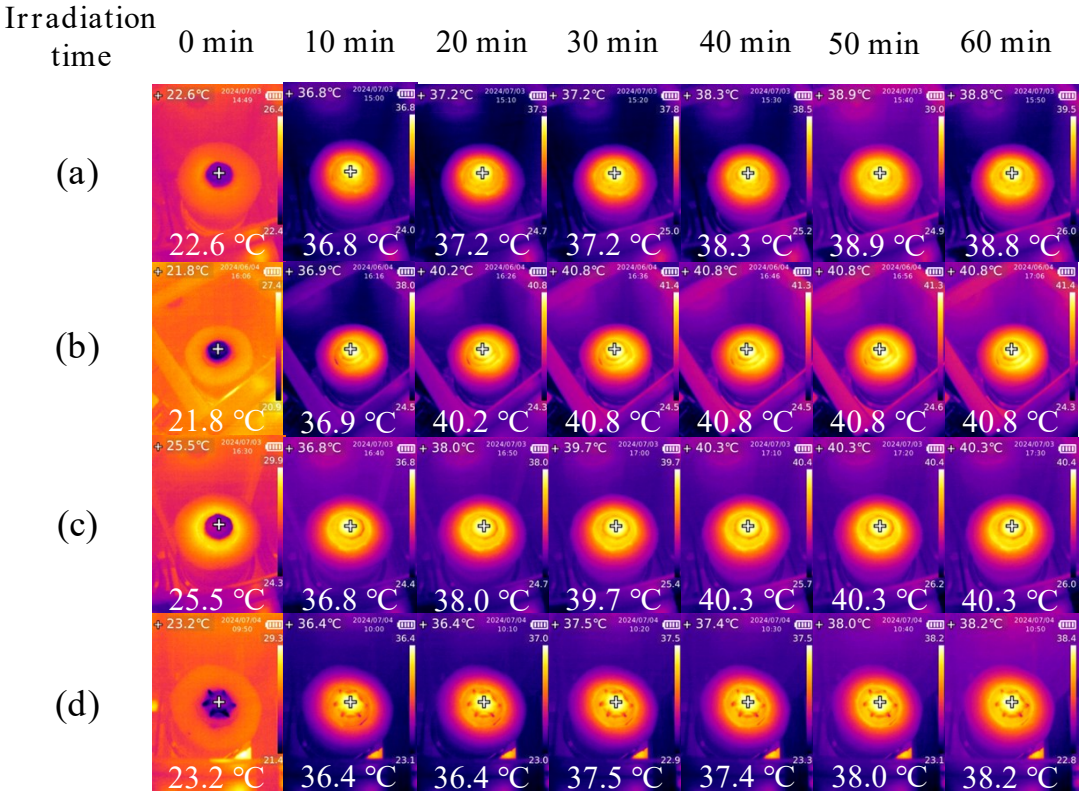

Figure S5. Infrared thermogram of the temperature changes of the round wet film anchored by (a) $Ni/Al_2O_3@Co_{400}$, (b) $NiAl_2O_3@Co_{500}$ and (c) $Ni/Al_2O_3@Co_{600}$ under sunlight at different temperatures. (d) Infrared thermogram of the temperature change of polygonal wet film composed of $Ni/Al_2O_3@Co_{500}$ under sunlight irradiation.

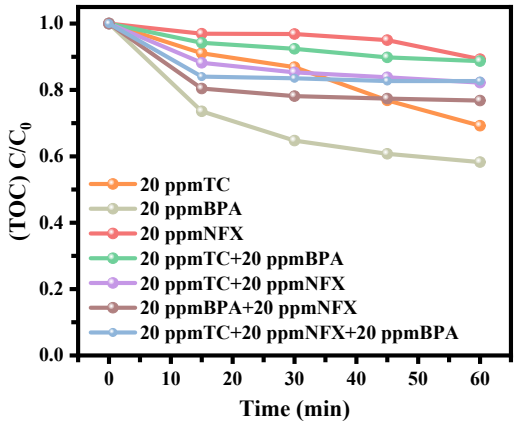

Figure S6. Mineralization of TC in $NiAl_2O_3@Co_{500}$/PMS system. Reaction conditions: [PMS] = 0.4 g L^{-1}, [catalyst] = 0.4 g L^{-1}, Temperature = 25 ℃.

Table S1. The proportion of elements in each surface element composition of the sample extracted by XPS.

Sample	Co			C		N		O		
	+2	+3	sat	C-C	C=O	Pyrrole	Pyridine	O_A	O_{UE}	O_L
$Ni/Al_2O_3@Co_{500}$	64.80	18.14	17.06	87.45	12.55	62.31	37.69	44.68	47.34	7.98
$Al_2O_3@Co_{500}$	54.93	22.31	22.76	90.81	9.19	49.74	50.26	12.90	74.34	12.76

Table S2. Surface elemental composition of samples extracted from XPS results.

Sample	**C Content (%)**	**N Content (%)**	**O Content (%)**	**Co Content (%)**	**Ni Content (%)**
$Ni/Al_2O_3@Co_{500}$	48.56	5.82	30.68	1.96	9.28
$Al_2O_3@Co_{500}$	18.89	2.17	50.36	0.93	0

Table S3. A summary of TC degradation performances in different heterogeneous catalyst/PMS systems.

Catalyst	Reaction conditions				Reaction time (min)	Degradation efficiency (%)	Reaction rate constant (min^{-1})	Ref
	TC (mg/L)	Catalyst (g/L)	PMS	Temperature (℃)				
$NiCo_2O_4$@C	10	0.1	0.8 mM	25	20	98.1	0.183	1
NiCo/CoNiO2@CNTs	20	0.2	1.3 mM	25	30	95.9	0.184	2
Co, Ni-100TACN	50	0.2	0.3 g/L	25	1	100	4.008	3
Co-FeNi-LDH	20	0.2	0.225 mM	25	5	100	1.288	4
Ni-Co-2H-MoS_2	20	0.15	0.5 mM	25	60	99.5	0.141	5
Ni/Al_2O_3@Co_{500}	20	0.4	0.4 g/L	25	20	98.6	0.498	This work

Table S4. Statistics results for evaporation rate and corresponding receiver efficiency of the $NiAl_2O_3@Co_{500}$ and other reported materials.

Photothermal Materials	Water Evaporation Rate (kg m^{-2} h^{-1})	PTCE (%)	References
$Ni/Al_2O_3@Co_{500}$	1.944	98.81	This work
$Co@SiO_2$/Cu-6	1.595	97.51	[6]
NiPS3/PVS	1.48	93.5	[7]
Od-V_2O_5	1.29	88.1	[8]
CCN	1.35	90.1	[9]
MoO_2-16h	1.777	92	[10]
SiO_2@Co/C-600	1.36	81.59	[11]
CoFe/ SiO_2-8	1.28	77.9	[12]
MS-Co-500N_2	1.15	69.82	[13]
GMW-3	1.58	87.2	[14]
PPy-E-Wood	1.35	86	[15]

References

1 Y. Chen, K. Zhu, W. Qin, Z. Jiang, Z. Hu, M. Sillanpää, K. Yan, *Chemical Engineering Journal* **2024**, *488*, 150786.

2 J. Zang, L. Chen, S. Zhong, G. Fan, *Journal of Environmental Chemical Engineering* **2024**, *12*, 113844.

3 J. Shi, Y. Xu, Y. Chen, W. Jiang, B. Liu, W. Pei, C. Liu, T. Zhou, G. Che, *Separation and Purification Technology* **2025**, *354*, 129492.

4 Y. Liu, H. Zhao, D. Wu, X. Shang, M. Lv, H. Yu, *Journal of Environmental Chemical Engineering* **2024**, *12*, 113723.

5 X. Song, S. Diao, W. He, J. Yang, L. Wang, G. Qin, Y. Li, Q. Chen, *Separation and Purification Technology* **2024**, *333*, 125927.

6 S. Wang, M. Liu, Y. Gao, H. Zhao, H. Zhu, R. Du, Y. Zheng, Z. Guo, Y. Wang, Y. Song, *ChemSusChem* **2024**, *17*, e202400406.

7 H. Wang, Y. Bo, M. Klingenhof, J. Peng, D. Wang, B. Wu, J. Pezoldt, P. Cheng, A. Knauer, W. Hua, *Advanced Functional Materials* **2024**, *34*, 2310942.

8 L. Wang, Y. Zeng, A. Huang, S. Zhang, *Journal of Solid State Chemistry* **2023**, *317*, 123718.

9 B. Zhang, H. Chen, Y. Huang, W.-M. Lau, D. Zhou, *Chemical Engineering Journal* **2023**, *468*, 143689.

10 T. Emrinaldi, M. A. Dwiputra, A. R. Fareza, A. A. Umar, F. A. A. Nugroho, R. T. Ginting, V. Fauzia, *Environmental Progress & Sustainable Energy* **2024**, *43*, e14234.

11 R. Du, H. Zhu, H. Zhao, H. Lu, C. Dong, M. Liu, F. Yang, J. Yang, J. Wang, J. Pan, *Journal of Alloys and Compounds* **2023**, *940*, 168816.

12 M. Liu, S. Ma, H. Zhao, H. Lu, J. Yang, S. Tang, S. Gao, F. Yang, *Journal of Alloys and Compounds* **2023**, *949*, 169901.

13 Y.-R. Gao, H.-Y. Zhao, M.-T. Liu, Q.-N. Liu, Y.-Y. Wang, L.-L. Li, J.-W. Yuan, Y.-Y. Song, F. Yang, *Rare Metals* **2024**, 1-17.

14 Y. Sun, S. Qiu, Z. Fang, J. Yang, X. Song, S. Xiao, *ACS Sustainable Chemistry & Engineering* **2023**, *11*, 3359-3369.

15 L. Shi, M. Zhang, X. Du, B. Liu, S. Li, C. An, *Journal of Materials Science* **2022**, *57*, 16317-16332.